

Supplementary Information for

Layered tin monoselenide as advanced photothermal conversion materials for efficient solar energy driven water evaporation

Jiandong Yao, Zhaoqiang Zheng and Guowei Yang*

State Key Laboratory of Optoelectronic Materials and Technologies, Nanotechnology
Research Center, School of Materials Science & Engineering, School of Physics &
Engineering, Sun Yat-sen University, Guangzhou 510275, Guangdong, P. R. China.

*Corresponding author: stsygw@mail.sysu.edu.cn

S1. Surface morphology of bare nickel foam substrate.

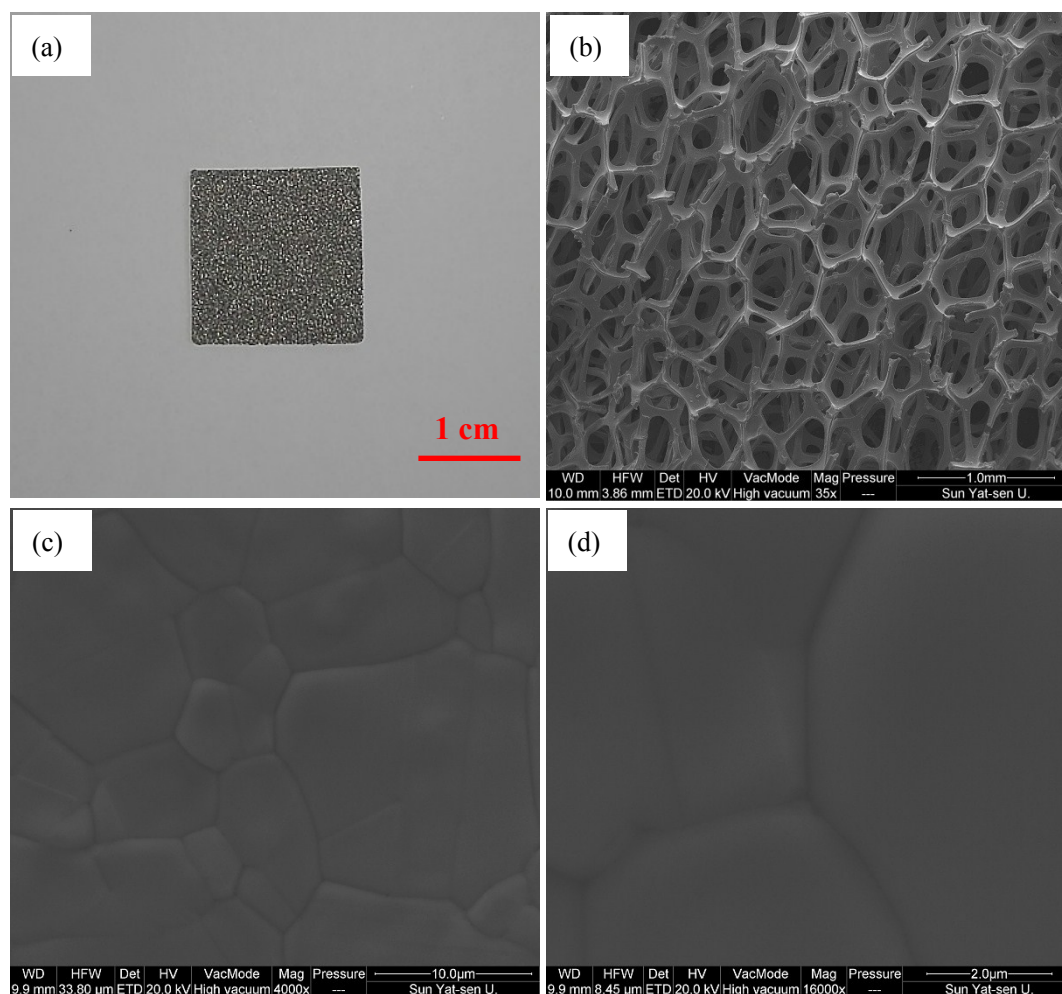


Figure S1. Morphology characterizations of bare nickel foam. (a) Digital photograph, scale bar: 1 cm. SEM images at different magnifications, (b) $35\times$, scale bar: 1 mm, (c) $4000\times$, scale bar: $10\ \mu\text{m}$, (d) $16000\times$, scale bar: $2\ \mu\text{m}$.

S2. Schematic diagram on growth dynamics of laterally/vertically aligned SnSe.

In general, PLD growth process includes nucleation, aggregation and growth. Due to sudden break of periodically arranged atoms, NF's surface possesses numerous arbitrarily distributed dangling bonds. They hinder lateral migration of surface atoms. As shown in Fig. S2(a), if nucleation occurs in positions with sparse dangling bonds, surrounding atoms are freely to migrate and attach to nucleus, leading to efficient lateral growth. In contrast, if nucleation occurs in positions with dense dangling bonds, it is difficult for nucleus to grow laterally due to obstruction of surrounding surface dangling bonds. Thus, in this case, growth is preferentially to be carried out in vertical direction, as shown in Fig. S2(b). As a result, the products contain both laterally and vertically aligned SnSe flakes.

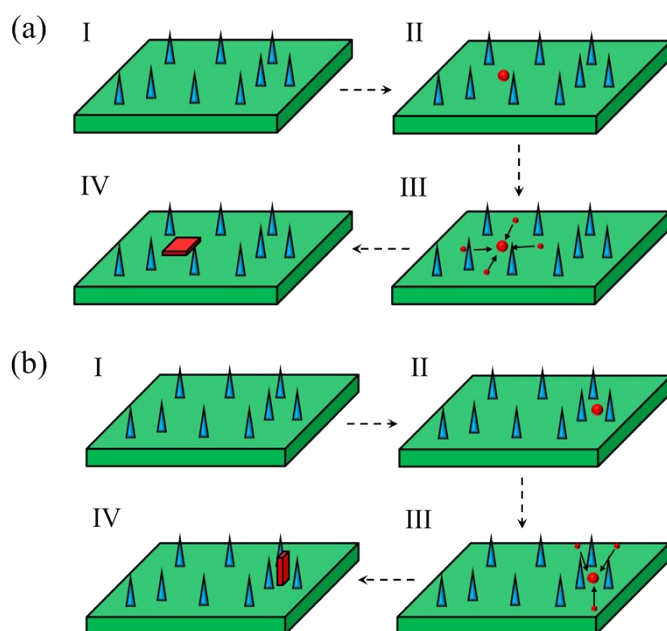


Figure S2. Schematic diagram illustrating growth mechanisms of SnSe with nucleus in positions with (a) sparse and (b) dense surface dangling bonds.

S3. Absorbance of sapphire (Al_2O_3) substrate.

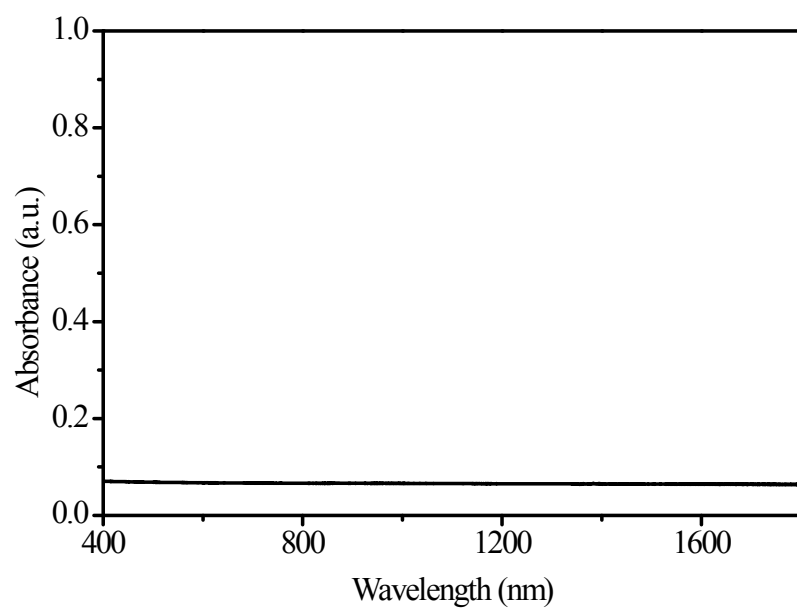


Figure S3. Absorbance of sapphire substrate in the solar spectrum range.

S4. Heating process of the SnSe@NF evaporation system.

To find out origin for enhancement of water evaporation, temperature trend of the evaporation system is monitored. The results are summarized in Fig. S4. As shown in Fig. S4(a), before irradiation, the whole container remains a uniform low temperature. After the irradiation is on, temperature of SnSe@NF device (bottom of container) increases first (Fig. S4(b)). And temperature of upper water remains relatively unchanged. As time goes by, high-temperature region gradually spreads from SnSe@NF device to its surrounding water and finally to the whole container (Fig. S4(c)-(h)). This process continues until the whole system reaches a uniform and high temperature (Fig. S4(i)). Therefore, the above heating process unambiguously affirms that enhancement of water evaporation is originated from efficient light harvesting of SnSe@NF device.

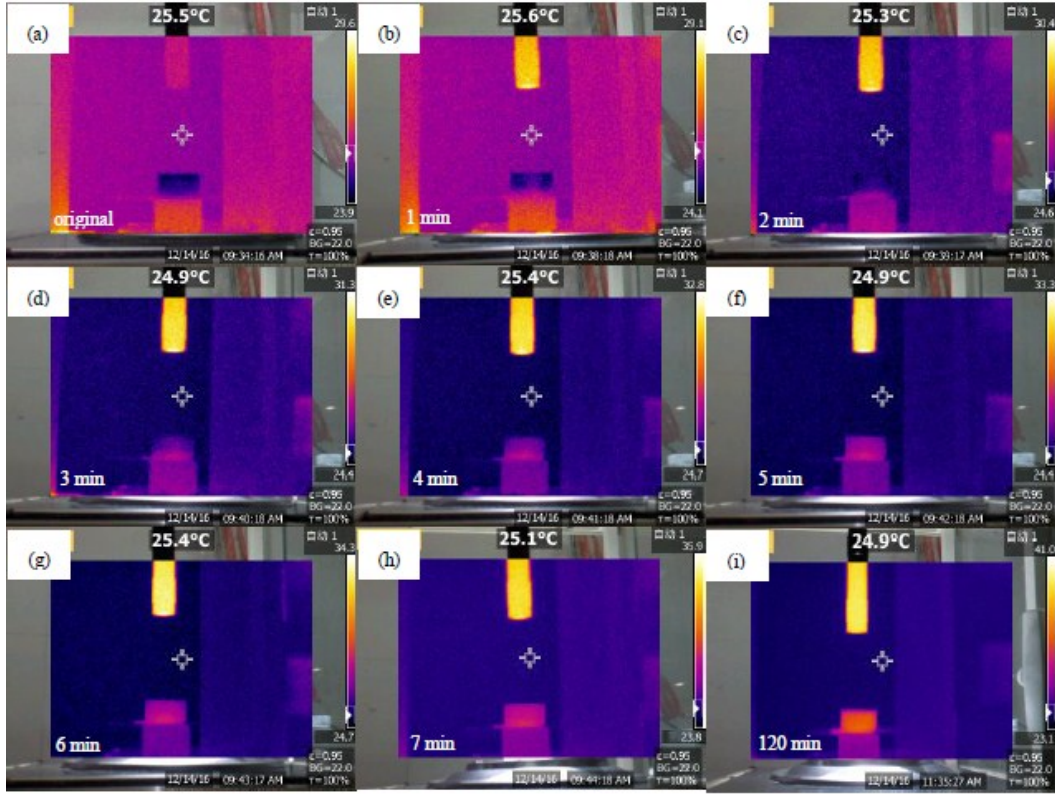


Figure S4. Photothermal mapping images of the SnSe@NF evaporation system upon AM 1.5 G solar irradiation for different periods. (a) Before irradiation. (b) 1 min. (c) 2 min. (d) 3 min. (e) 4 min. (f) 5 min. (g) 6 min. (h) 7 min. (i) 120 min. Power density: 100 mW/cm².

S5. Pulse number dependent thickness of the PLD-grown SnSe.

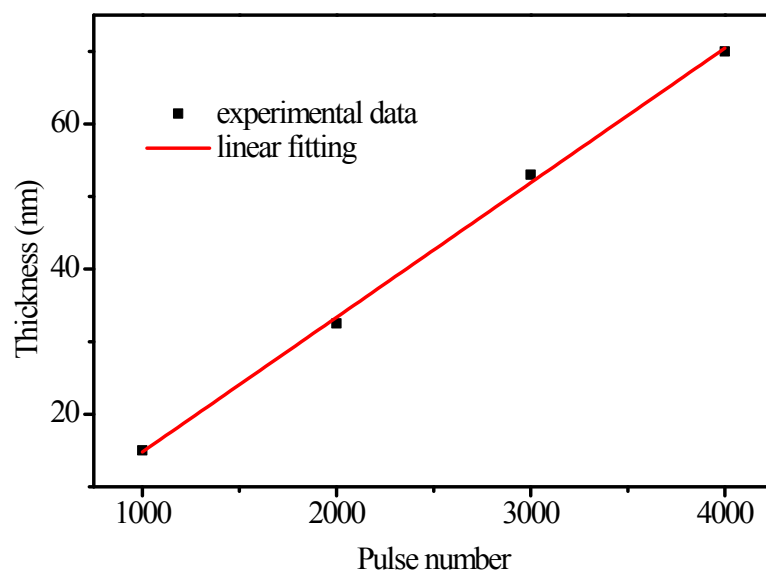


Figure S5. Pulse number dependent thickness of the PLD-grown SnSe.

S6. Time dependent mass loss curves with different water surface-device distances.

Fig. S6 presents time dependent mass loss curves with different water surface-device distances, including 1, 5 and 10 mm. Obviously, when device is still far away from water's surface, evaporation rate just increases slightly with decrease of water surface-device distance. When device is near surface of water, evaporation rate is significantly increased.

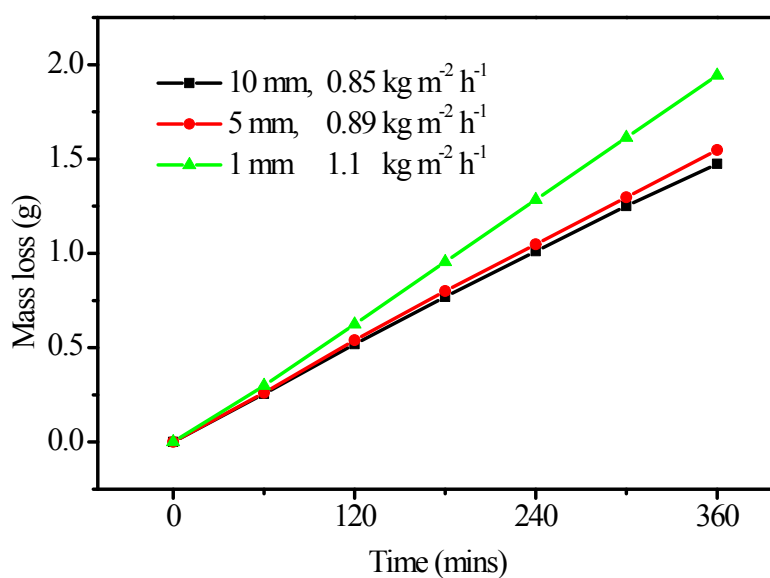


Figure S6. Time dependent mass loss curves with water surface-device distances of 1 (green), 5 (red) and 10 mm (black).

S7. Optical properties of SnSe/Al₂O₃ and SnSe@NF.

Fig. S7 presents absorption spectrums of SnSe/Al₂O₃ (black) and SnSe@NF (red), respectively. Obviously, the SnSe@NF exhibits a much stronger absorbance. It is attributed to the multi-scattering induced light trapping, which is originated from the rough morphology of NF substrate.

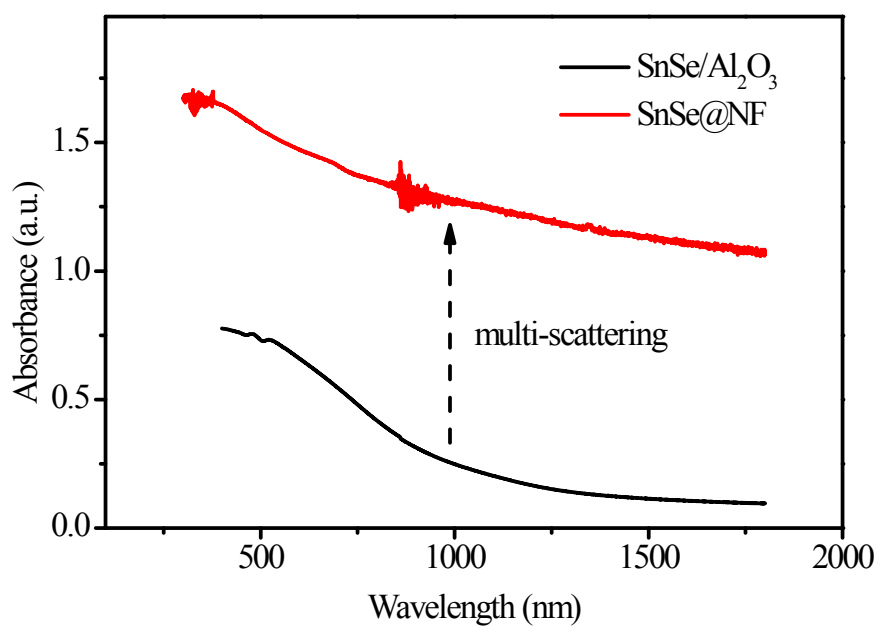


Figure S7. UV-Vis absorption spectrums of SnSe/Al₂O₃ and SnSe@NF.

S8. SEM images of SnSe@NF with different deposition pulse number.

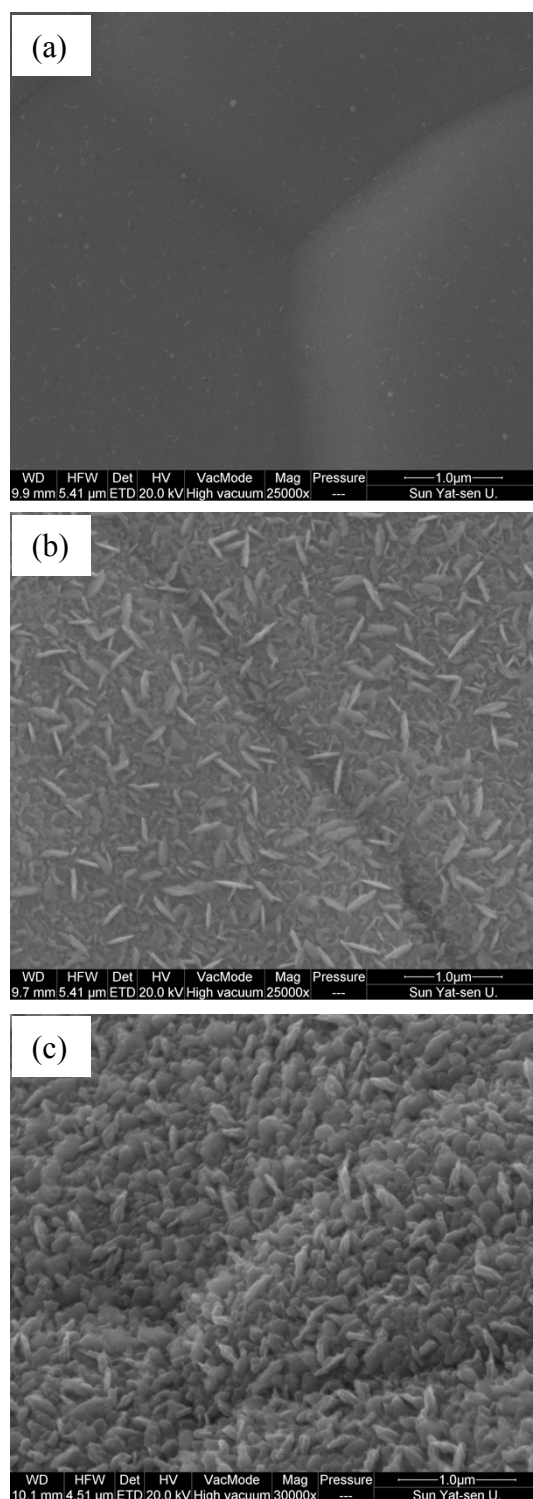


Figure S8. SEM images of SnSe@NF with different deposition pulse number. (a) 1000, (b) 4000, (c) 8000.